Room-temperature superconductivity in boron- and nitrogen-doped lanthanum superhydride

Yanfeng Ge [1], Fan Zhang [2,*] and Russell J. Hemley [3,*]

[1] *State Key Laboratory of Metastable Materials Science and Technology & Key Laboratory for Microstructural Material Physics of Hebei Province, School of Science, Yanshan University, Qinhuangdao 066004, China*

[2] *Department of Physics, University of Texas at Dallas, Richardson, Texas 75080, USA*

[3] *Departments of Physics, Chemistry, and Earth and Environmental Sciences, University of Illinois Chicago, Chicago, Illinois 60607, USA*

(Received 4 January 2021; revised 13 June 2021; accepted 29 November 2021; published 15 December 2021)

Recent theoretical and experimental studies of hydrogen-rich materials at megabar pressures (i.e., >100 GPa) have led to the discovery of very high-temperature superconductivity in these materials. Lanthanum superhydride LaH_{10} has been of particular focus as the first material to exhibit a superconducting critical temperature (T_c) near room temperature. Experiments indicate that the use of ammonia borane as the hydrogen source can increase the conductivity onset temperatures of lanthanum superhydride to as high as 290 K. Here we examine the doping effects of B and N atoms on the superconductivity of LaH_{10} in its fcc ($Fm\bar{3}m$) clathrate structure at megabar pressures. Doping at H atomic positions strengthens the H_{32} cages of the structure to give higher phonon frequencies that enhance the Debye frequency and thus the calculated T_c. The predicted T_c can reach 288 K in $LaH_{9.985}N_{0.015}$ within the average high-symmetry structure at 240 GPa. The remarkably large shift in T_c to higher values produced by small degrees of chemical doping opens the prospect for the creation of still higher-temperature superconductivity in superhydrides potentially at even lower-pressure conditions.

DOI: 10.1103/PhysRevB.104.214505

Realizing room-temperature superconductivity in hydrogen-rich materials under pressure is a topic of great current interest. Specifically, high-pressure experiments motivated by density functional theory and Bardeen-Cooper-Schrieffer (BCS) theory have uncovered new classes of hydrogen-rich metal hydrides, or superhydrides, with superconducting critical temperatures (T_c's) in the vicinity of room temperature at megabar pressures (i.e., >100 GPa) [1,2]. Calculations for the rare-earth hydrides predicted that LaH_{10} and YH_{10} would form dense hydride clathrate structures exhibiting T_c's of 257–326 K at pressures of 200–300 GPa [3,4]. X-ray diffraction experiments on the La-H system confirmed the formation and stability of the LaH_{10} structure near the predicted pressures [5], and subsequent electrical conductivity and critical current measurements confirmed the very high-temperature superconductivity of the phase [6,7]. Experiments that used ammonia borane (NH_3BH_3) as the hydrogen source indicated T_c's beginning at 260 K, including conductivity onsets as high as 290 K that have been observed in recent work [8]. It was proposed that the high and variable T_c arises from incorporation of N and/or B in the structure from the ammonia borane starting material [7,8]. Moreover, subsequent study [9] that confirmed the reported structure [10] and high-temperature superconductivity [7,8] of LaH_{10} found a slightly lower maximum T_c of 250 K in experiments conducted without ammonia borane.

Using a theoretical method successfully applied previously to H_3S [11,12], here we show that B and N doping increases the T_c of the lanthanum-based superhydride to room temperature. It is found that the doping at H atomic position makes the clathrate hydride structure more stable and hardens the low-frequency optical phonons. Although the electron-phonon coupling constant λ is reduced, a marked increase of the logarithmically averaged phonon frequency $\langle\omega\rangle_{\log}$, equivalent to the rise of Debye temperature, enhances T_c. Remarkably, low-level doping of N in the H sublattice together with further increase in pressure raises the T_c of LaH_{10} by at least 25 K, with a predicted T_c for $LaH_{9.985}N_{0.015}$ at 240 GPa of 288 K.

The electron-phonon coupling was studied with the linear response theory and the Migdal-Eliashberg approach [13–16]. The Eliashberg electron-phonon spectral function reads

$$\alpha^2F(\omega) = \frac{1}{2\pi N(\epsilon_F)} \sum_{\boldsymbol{q},\nu} \frac{\gamma_{\boldsymbol{q},\nu}}{\omega_{\boldsymbol{q},\nu}} \delta(\omega - \omega_{\boldsymbol{q},\nu}), \tag{1}$$

where $N(\epsilon_F)$ is the density of states (DOS) per spin at the Fermi level and $\gamma_{\boldsymbol{q},\nu}$ is the phonon linewidth given by the Fermi's golden rule,

$$\gamma_{\boldsymbol{q},\nu} = 2\pi\omega_{\boldsymbol{q},\nu} \sum_{i,j,\boldsymbol{k}} \left|M^{\boldsymbol{q},\nu}_{i\boldsymbol{k},j\boldsymbol{k}+\boldsymbol{q}}\right|^2 \delta(\epsilon_{i\boldsymbol{k}} - \epsilon_F)\delta(\epsilon_{j\boldsymbol{k}+\boldsymbol{q}} - \epsilon_F). \tag{2}$$

The microscopic electron-phonon matrix element $M^{\boldsymbol{q},\nu}_{i\boldsymbol{k},j\boldsymbol{k}+\boldsymbol{q}}$ describes the scattering of an electron at the Fermi surface from a state of momentum $\boldsymbol{k}$ to another state of $\boldsymbol{k}+\boldsymbol{q}$ perturbed by a phonon mode $(\boldsymbol{q},\nu)$. In the electron-phonon coupling model, the superconducting state is obtained by solving the Eliashberg gap equation with the electron-phonon and electron-electron interactions in the normal state. Describing the manifestation of electron-phonon interaction in superconductivity, the electron-phonon coupling constant λ was

*Corresponding authors: zhang@utdallas.edu; rhemley@uic.edu

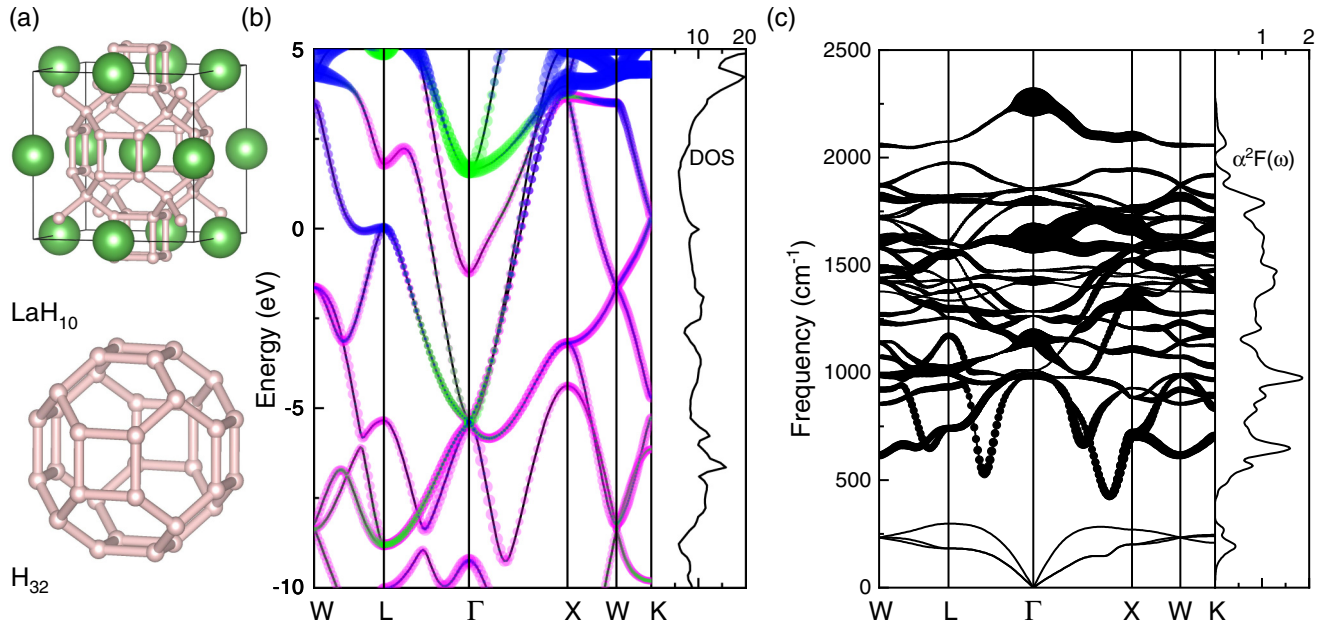

FIG. 1. (a) Optimized structure of LaH_{10} with its fcc La sublattice and H_{32} clathrate structure. (b) Electronic band structure and DOS (Hartree^{-1}/spin) of LaH_{10} at 210 GPa. (c) Phonon dispersion and Eliashberg function $\alpha^2F(\omega)$ of LaH_{10} at 210 GPa. The pink, blue, and green circles in (b) mark the projections of H-*s*, La-*d*, and La-*f* orbitals, respectively. The size of the black circles in (c) is proportional to the electron-phonon coupling linewidths. The results are consistent with the original predictions [3].

obtained from $\lambda = 2\int \alpha^2F(\omega)\omega^{-1}d\omega$. The electron-electron Coulomb interaction was represented by an effective constant μ^*. The T_c was estimated by the Allen-Dynes-modified McMillan formula [16]

$$T_c = f_1 f_2 \frac{\langle\omega\rangle_{\log}}{1.20}\exp\left[-\frac{1.04(1+\lambda)}{\lambda-\mu^*(1+0.62\lambda)}\right], \qquad (3)$$

where f_1 and f_2 are the strong coupling and shape correction factors, respectively, and $\langle\omega\rangle_{\log}$ is the logarithmically averaged phonon frequency.

The technical details of the computation are as follows. Density functional theory was implemented within the generalized gradient approximation using the Perdew-Burke-Ernzerh method in the ABINIT package [17–19]. The ion and electron interactions were treated with the Hartwigsen-Goedecker-Hutter pseudopotentials [20]. The basis set containing all plane waves up to the cutoff energy of 30 Hartree and the zone-centered Monkhorst-Pack k mesh of 24×24×24 were used in all calculations. The phonon spectra and electron-phonon coupling were calculated on an 8×8×8 q grid using the density functional perturbation theory [21]. For electron-phonon coupling, the matrix elements were determined by second-order perturbation theory. To improve accuracy we performed a Fourier interpolation of the matrix elements to obtain them on a finer q grid identical to the k mesh. The doping of B and N atoms was simulated by the self-consistent virtual crystal approximation (VCA), where the pseudopotentials of $A_{1-x}B_x$ are given by $(1-x)V_A + xV_B$.

Lanthanum superhydride, LaH_{10}, has been found to be the highest temperature superconducting phase so far in the La-H binary system. As a result, since the original theoretical prediction and experimental discovery [3–7], the material has been the subject of numerous investigations (e.g., Refs. [22–29]). Though the detailed properties of LaH_{10}, including anharmonicity and nuclear quantum effects, continue to be studied theoretically [10,22–28], it is sufficient for the present purposes to examine its superconducting properties, and specifically, the nature of the electron-phonon coupling in the system, within a conventional quasiharmonic treatment of the lattice dynamics. The computational approach applied here is consistent with previous theoretical studies [3,4], which have been largely confirmed by experimental results for lanthanum superhydride [3–7], thereby validating the extensions of the techniques we use to examine the effects of doping, as described previously [11,12].

The high-symmetry clathrate-type structure of LaH_{10} consists of La atoms arrayed on an fcc lattice (space group $Fm\bar{3}m$), with a 32-atom hydrogen (H_{32}) cage surrounding each La atom containing six square and twelve hexagonal faces that are cross linked by eight hydrogen cubes [Fig. 1(a)]. The central La atom acts as an electron source, donating electrons to the H sublattice, a result consistent with the ambient pressure ionization potential of La [27]. The electron transfer destabilizes molecular H_2 units in the structure that form in pure solid hydrogen at these pressures. This strong anion-cation interaction also enhances the stability of the H_{32} cage, which is predicted to be dynamical unstable in La_0H_{10} [28].

We focus on the properties of the material at pressures where the T_c has a maximum for pure LaH_{10}, which corresponds to 210 GPa and close to the calculated quasiharmonic dynamical instability of the fcc structure [3,10]. The calculated nearest-neighbor H-H distances are 1.09 and 1.17 Å at this pressure, consistent with previous work [3,4]. Figure 1(b) shows that LaH_{10} is a good metal, and the holelike and electronlike bands around the L point generate a van Hove

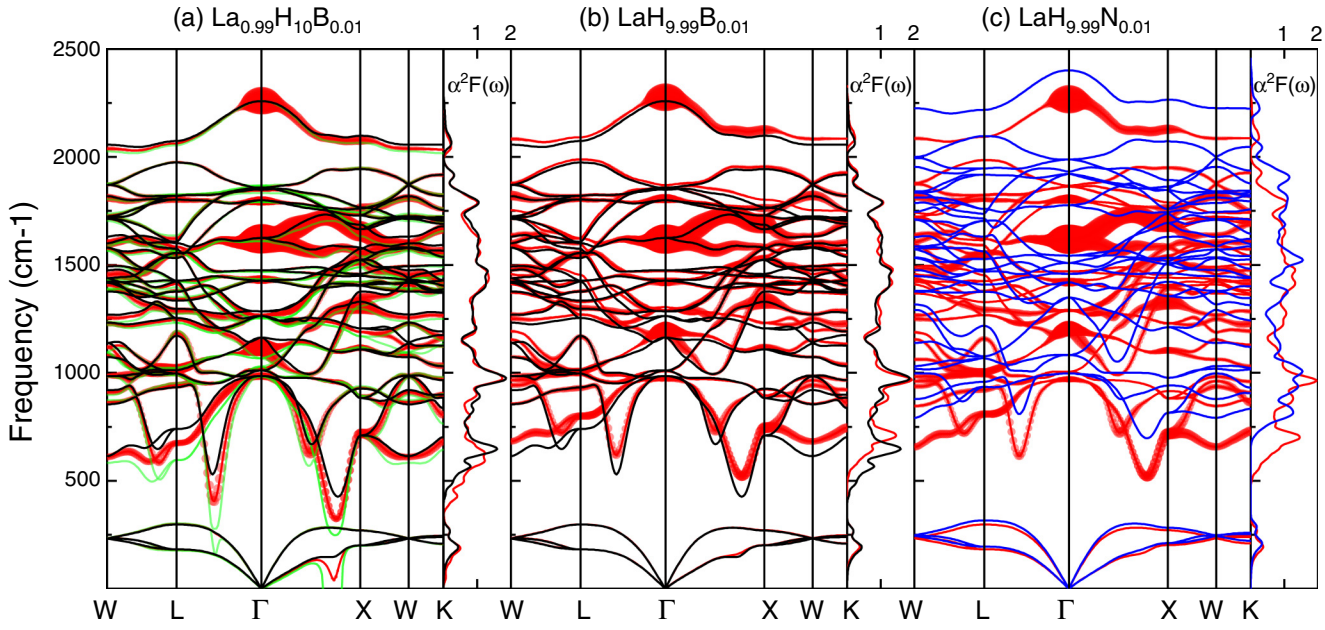

FIG. 2. Phonon dispersion (red lines) and Eliashberg function $\alpha^2F(\omega)$ (red lines) of (a) $La_{0.99}H_{10}B_{0.01}$, (b) $LaH_{9.99}B_{0.01}$ and (c) $LaH_{9.99}N_{0.01}$ at 210 GPa. The size of red circles is proportional to the electron-phonon coupling linewidths. In order to facilitate the comparison, the black lines in (a), (b) show the phonon disperson and $\alpha^2F(\omega)$ of LaH_{10} at 210 GPa. The green lines in (a) show the phonon dispersion of $La_{0.98}H_{10}B_{0.02}$ at 210 GPa with the imaginary modes along Γ-X. The blue lines in (c) show the phonon dispersion and $\alpha^2F(\omega)$ of $LaH_{9.99}N_{0.01}$ at 240 GPa.

singularity near the Fermi energy [27]. This peak in the electronic DOS near the Fermi level reaches 10.77 Hartree^{-1}/spin, and arises mainly from La-d, La-f, and H-s electrons. Phonon calculations reveal no imaginary frequencies indicating quasiharmonic dynamical stability of the $Fm\bar{3}m$ structure at 210 GPa [Fig. 1(c)]. On the other hand, at this pressure the structure is close to a dynamical instability, as indicated by the mode softening along Γ-L and Γ-X, which is associated with the maximum T_c calculated at this level of theory for pure LaH_{10} [3,10]. The H-H distances lead to mixing of stretching and bending vibrations [3], and phonon modes dominated by this H motion contribute to the electron-phonon coupling. As a result, the electron-phonon couplings, as reflected in the phonon linewidths, are distributed across many optical phonons [Fig. 1(c)]. The Allen-Dynes-modified McMillan formula gives a $T_c = 261$ K for LaH_{10} at 210 GPa with $\lambda = 2.96$, $\langle\omega\rangle_{\log} = 1090$ K, and $\mu^* = 0.11$. In addition, T_c drops with increasing pressure because the enhancement due to the increase in $\langle\omega\rangle_{\log}$ is counteracted by the stronger negative effect due to the drop in λ [30]. Both the T_c values and trends agree with previous theoretical results [30], and the T_c is close to the experimental findings [3,6,9,22,23,27] (Fig. S1) [30]. Because of the slight differences in the absolute value of the calculated T_c that arise from different codes and parameters (e.g., μ^*) used in previous work (Fig. S1), to examine the effect of doping we adopt the above value of T_c for pure LaH_{10} at 210 GPa as a reference and use the same formalism for all the calculations while also examining the dependence of the results on μ^*.

Experimental studies have suggested that incorporation of N and/or B can improve the superconductivity of LaH_{10} [8]. Over the range of conditions explored to date, there is no evidence for major structural changes from cubic to higher pressure P-T structures. Thus, we consider the effects of modest doping of B and N, without structural phase transition, on the electron distribution, structural stability, and superconductivity of the fcc LaH_{10}. We compare the results between $La_{0.99}H_{10}B_{0.01}$ and $LaH_{9.99}B_{0.01}$ at 210 GPa. Considering first the former, since B has many fewer valence electrons than La, the predominant effect of doping to create a virtual $La_{0.99}B_{0.01}$ atom is reduced electron transfer to the H atom framework. This weakens the H_{32} cages as indicated by phonon softening shown in Fig. 2(a). Notably, frequencies of acoustic phonons along Γ-X become imaginary with modest doping, as indicated for $La_{0.98}H_{10}B_{0.02}$. By contrast, due to the increase in valence electrons of the virtual $H_{9.99}B_{0.01}$ atom, phonon hardening and notable changes in phonon frequencies around 500 cm^{-1} occur [Fig. 2(b)]. The two types of doping result in phonon linewidths that are close to those of the LaH_{10} prototype. This minor change in electron-phonon coupling arises from the similarity in the DOS at the Fermi level (10.57 and 10.80 Hartree^{-1}/spin for $La_{0.99}H_{10}B_{0.01}$ and $LaH_{9.99}B_{0.01}$, respectively), which is distinctly different from the doping effect found for H_3S [11,12]. Consequently, the peaks in the Eliashberg functions $\alpha^2F(\omega)$ change little, though the peaks around 500 cm^{-1} shift [Figs. 2(a) and 2(b)]. With the low-frequency optical phonon softening, λ of $La_{0.99}H_{10}B_{0.01}$ is enhanced but $\langle\omega\rangle_{\log}$ is reduced. The calculated T_c is 245 K with $\lambda = 3.33$, $\langle\omega\rangle_{\log} = 900$ K, and $\mu^* = 0.11$. By contrast, the effect is the opposite for $LaH_{9.99}B_{0.01}$, with $\lambda = 2.66$ and $\langle\omega\rangle_{\log} = 1180$ K, and the calculated T_c is 269 K, i.e., the T_c is increased relative to LaH_{10} and $La_{0.99}H_{10}B_{0.01}$ because of phonon hardening.

The above results indicate that superconductivity of fcc LaH_{10} is enhanced by increasing the stability of H_{32} cage structure with additional charge transfer from the metal atom to the hydrogen framework. For this reason, we focus on

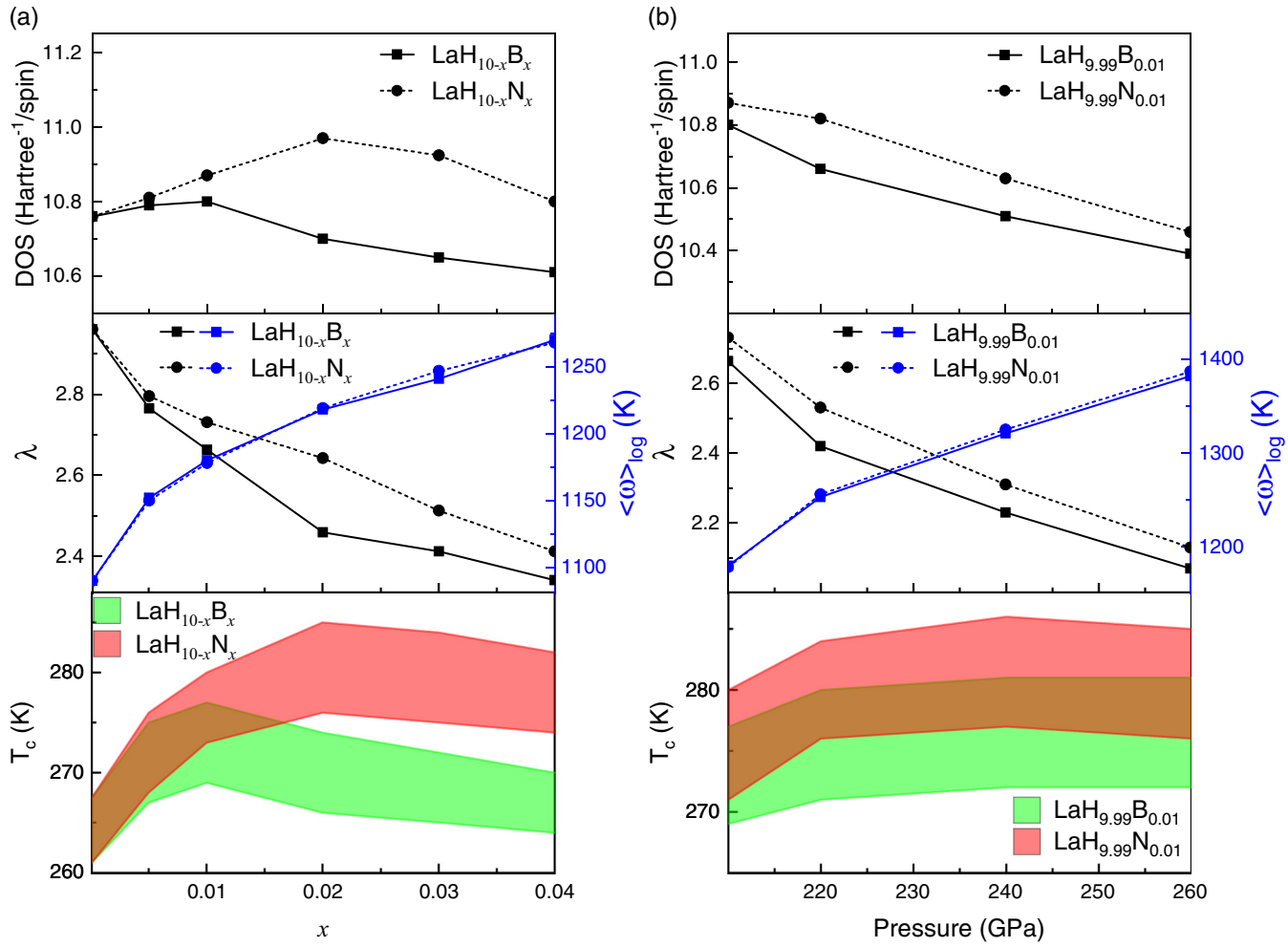

FIG. 3. (a) DOS, λ, $\langle\omega\rangle_{log}$, and T_c of $LaH_{10-x}B_x$ and $LaH_{10-x}N_x$ with different doping levels at 210 GPa. (b) DOS, λ, $\langle\omega\rangle_{log}$, and T_c of $LaH_{9.99}B_{0.01}$ and $LaH_{9.99}N_{0.01}$ at different pressures. For each T_c curve, the upper and lower bounds are obtained by choosing $\mu^* = 0.10$ and 0.11, respectively.

the doping of B and N in the H sublattice (Fig. 3). Such doping results in small changes in the calculated DOS with doping level $x \leqslant 0.04$ for both $LaH_{10-x}B_x$ and $LaH_{10-x}N_x$, as shown in Fig. 3(a). Rising phonon frequencies after doping of B or N cause λ ($\langle\omega\rangle_{log}$) to decrease (increase), whereas the phonon linewidths show less of a change. According to the BCS theory, strong electron-phonon coupling and high Debye frequency increase T_c. It turns out that the increase of $\langle\omega\rangle_{log}$ in $LaH_{10-x}B_x$ and $LaH_{10-x}N_x$ can offset the negative effect of the lower λ and thus increase T_c. The larger DOS at the Fermi level imparts a slightly stronger electron-phonon coupling and higher T_c for $LaH_{10-x}N_x$ compared to $LaH_{10-x}B_x$ at a fixed doping level. Notably, the calculated T_c of $LaH_{9.98}N_{0.02}$ is 276 (285) K with $\mu^* = 0.11$ (0.10) [31]. Moreover, we performed supercell calculations to test the validity of these VCA predictions [30]. The calculated electronic DOS, phonon spectrum, and T_c from the supercell simulations all support the VCA results for N-doped LaH_{10} described above (Figs. S2 and S3) [30]. We note that the validity of the VCA decreases with increasing doping levels, but at the low levels studied here (<5%) the VCA is valid, e.g., as a background-charge approximation.

We also studied pressure effects on the B and N doping in the hydrogen framework. Pressure compresses the H-H bonds, thereby increasing the frequencies of H atomic vibrations. As a result, there is an overall blue shift in the higher frequency portion of the Eliashberg function [Fig. 2(c)], which significantly differs from the effects of doping that largely changes the lower frequency optical phonons. Because of the holelike and electronlike bands around the Fermi level, a weakly pressure-dependent DOS also gives rise to a small variation of phonon linewidths. As illustrated for $LaH_{9.99}B_{0.01}$ and $LaH_{9.99}N_{0.01}$ in Fig. 3(b), the effect of pressure is similar to that of doping and leads to a limited boost in T_c.

The dependence of T_c on both doping level and pressure for $LaH_{10-x}N_x$ is shown in Fig. 4. The results indicate the predicted upper limit of T_c by N doping while preserving the dynamically stable fcc LaH_{10} structure. With $\mu^* = 0.10$ (0.11), the T_c is calculated to reach 288 (278) K for $LaH_{9.985}N_{0.015}$ at 240 GPa and $\lambda = 2.26$ and $\langle\omega\rangle_{log} = 1330$ K. The results indicate an increase in T_c of over 25 K compared to the maximum T_c calculated at the same level of theory for LaH_{10} (i.e., 261 K at 210 GPa). Therefore, remarkably small

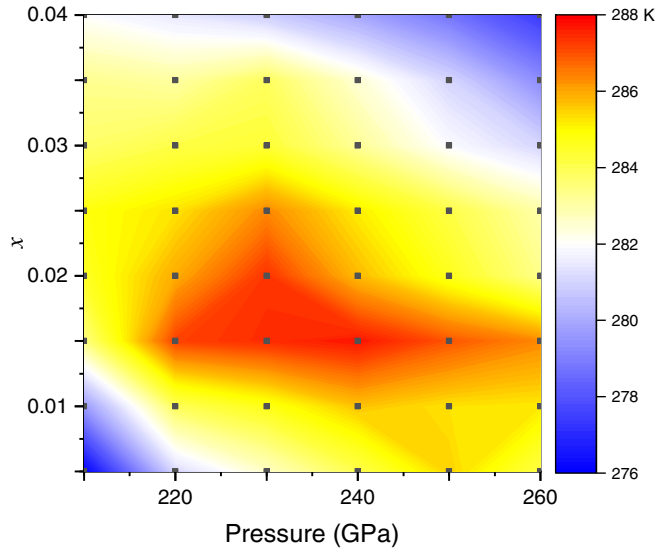

FIG. 4. Dependence of T_c on doping level and pressure for $LaH_{10-x}N_x$ with $\mu^* = 0.10$. The black dots represent the calculated data grid.

doping levels are able to raise the calculated T_c to the vicinity of room temperature. Although the inclusion of anharmonicity and other quantum effects could shift the predicted T_c, the very low doping level here suggests that the effect would be similar to that predicted when these effects are included for pristine LaH_{10} [23]; thus, the shift in T_c due to N doping is expected to be similar to that found here.

Remarkably strong effects of chemical doping on T_c are predicted by our calculations. Specifically, very low doping levels are able to shift T_c's to higher values as we found hole doping by carbon in H_3S causes a marked increase in T_c to room temperature [12], in agreement with the critical temperature of 288 K reported for a C-S-H mixture at 270 GPa [32]. While experimental evidence for such doping is challenging at these multimegabar pressures, theory can help guide experimental tests of these effects. For example, additional x-ray diffraction lines were observed in LaH_{10} experiments in which the temperature was nominally increased above that required to synthesize the decahydride [6], and additional splittings have been found in a more recent study of the material that involved subsequent thermal annealing [8]. It is thus plausible that N/B can readily be incorporated in the LaH_{10} structure upon heating, even below the temperature required for additional stoichiometric compounds to form [6]. Notably, this substitution would not appreciably change the measured diffraction pattern, but merely shift peaks and unit-cell volumes at the same pressure relative to LaH_{10} [6]. In addition, if the doping produces an ordered (or partially ordered) phase, satellite peaks would appear near the main peaks, as explicitly calculated here for the $La_8H_{79}N$ supercell (Fig. S4) [30]; new low-frequency modes would also be observed in Raman or infrared spectra, also as predicted by these calculations (Fig. S3) [30]. In principle, high-pressure *K*-edge x-ray Raman measurements (e.g., of N and B [33]) could also constrain the nature and degree of doping.

In summary, we have systematically studied the doping effects of B and N on the superconductivity of LaH_{10} at megabar pressures, including the doping at La and H atomic positions. It is found that doping at the H positions stabilizes the clathrate hydride structure and hardens the low-frequency optical phonons. Although the electron-phonon coupling constant λ is reduced, the marked increase in the effective Debye temperature $\langle\omega\rangle_{\log}$ offsets the effect to increase the calculated T_c's. As noted above, the effect of doping on T_c's thus differs from that found previously for doping of H_3S with P, Si, and C, which arose principally from changes in DOS at the Fermi level [11,12]. The results provide an explanation for the room-temperature superconductivity up to 290 K reported in several experiments on lanthanum superhydrides conducted using NH_3BH_3 as a hydrogen source [6–8,29]. A recently reported theoretical study of doping of LaH_{10} suggested enhancing T_c exclusively through the effect on the DOS [34], similar to our predictions for H_3S [11,12]. By contrast, the calculations presented here show that doping can enhance T_c in other ways, e.g., by increasing the Debye frequency. Still higher T_c's may be possible in the La-based system as a result of doping combined with structural changes induced by further application of pressure and temperature [8]. Electron- or hole-doping with other elements in rare-earth and other hydrides is likely to lead to still higher T_c's in hydrides as suggested by recent theoretical calculations on the Li-Mg-H system [35,36]. The results presented here should motivate and guide the design and interpretation of new experiments. Continued experimental and theoretical studies of doping effects and more complex chemical compositions of hydrides and related low-*Z* materials are expected to lead to very high-temperature superconductors that are recoverable at or near ambient pressure [37–39].

We thank M. Ahart, R. Kumar, N. Salke, and A. Haseeb for useful discussions. This work was supported by National Natural Science Foundation of China (Grant No.11904312), the UT Dallas Research Enhancement Fund, the U.S. National Science Foundation (Grant No. DMR-1933622), and the U.S. Department of Energy (Grants No. DE-SC0020340 and No. DE-NA0003975).

[1] T. Bi, N. Zafiri, T. Terpstra, and E. Zurek, The search for superconductivity in high pressure hydrides, in *Reference Chemistry Molecular Sciences and Chemical Engineering* (Elsevier, Amsterdam, 2019).

[2] J. A. Flores-Livas, L. Boeri, A. Sanna, G. Profeta, R. Arita, and M. Eremets, A perspective on conventional high-temperature superconductors at high pressure: Methods and materials, Phys. Rep. **856**, 1 (2020).

[3] H. Liu, I. I. Naumov, R. Hoffmann, N. W. Ashcroft, and R. J. Hemley, Potential high-T_c superconducting lanthanum and yttrium hydrides at high pressure, Proc. Natl. Acad. Sci. USA **114**, 6990 (2017).

[4] F. Peng, Y. Sun, C. J. Pickard, R. J. Needs, Q. Wu, and Y. Ma, Hydrogen Clathrate Structures in Rare Earth Hydrides at High Pressures: Possible Route to Room-Temperature Superconductivity, Phys. Rev. Lett. **119**, 107001 (2017).

[5] Z. M. Geballe, H. Liu, A. K. Mishra, M. Ahart, M. Somayazulu, Y. Meng, M. Baldini, and R. J. Hemley, Synthesis and stability of lanthanum superhydrides, Angew. Chem. Inter. Ed. **57**, 688 (2018).

[6] M. Somayazulu, M. Ahart, A. K. Mishra, Z. M. Geballe, M. Baldini, Y. Meng, V. V. Struzhkin, and R. J. Hemley, Evidence for Superconductivity above 260 K in Lanthanum Superhydride at Megabar Pressures, Phys. Rev. Lett. **122**, 027001 (2019).

[7] R. J. Hemley, M. Ahart, H. Liu, and M. Somayazulu, Road to room-temperature superconductivity: T_c above 260 K in lanthanum superhydride under pressure, in *Superconductivity and Pressure: A Fruitful Relationship on the Road to Room Temperature Superconductivity, Madrid, Spain, May 21–22, 2018*, edited by M. A. Alario-Franco (Fundación Ramón Areces, Madrid, Spain, 2019), pp. 199–213.

[8] A. D. Grockowiak, M. Ahart, T. Helm, W. A. Coniglio, R. Kumar, K. Glazyrin, G. Garbarino, Y. Meng, M. Oliff, V. Williams, N. W. Ashcroft, R. J. Hemley, M. Somayazulu, and S. W. Tozer, Possible superconductivity beyond 500 K in a La-based superhydride, arXiv:2006.03004.

[9] A. P. Drozdov, P. P. Kong, V. S. Minkov, S. P. Besedin, M. A. Kuzovnikov, S. Mozaffari, L. Balicas, F. Balakirev, D. Graf, V. B. Prakapenka, E. Greenberg, D. A. Knyazev, M. Tkacz, and M. I. Eremets, Superconductivity at 250 K in lanthanum hydride under high pressures, Nature (London) **569**, 528 (2019).

[10] H. Liu, I. I. Naumov, Z. M. Geballe, M. Somayazulu, J. S. Tse, and R. J. Hemley, Dynamics and superconductivity in compressed lanthanum superhydride, Phys. Rev. B. **98**, 100102(R) (2018).

[11] Y. Ge, F. Zhang, and Y. Yao, First-principles demonstration of superconductivity at 280 K in hydrogen sulfide with low phosphorus substitution, Phys. Rev. B **93**, 224513 (2016).

[12] Y. Ge, F. Zhang, R. P. Dias, R. J. Hemley, and Y. Yao, Hole-doped room-temperature superconductivity in $H_3S_{1-x}Z_x$ (Z = C, Si), Mater. Today Phys. **15**, 100330 (2020).

[13] W. L. McMillan, Transition temperature of strong-coupled superconductors, Phys. Rev. **167**, 331 (1968).

[14] P. B. Allen, Neutron spectroscopy of superconductors, Phys. Rev. B **6**, 2577 (1972).

[15] P. B. Allen and R. Silberglitt, Some effects of phonon dynamics on electron lifetime, mass renormalization, and superconducting transition temperature, Phys. Rev. B **9**, 4733 (1974).

[16] P. B. Allen and R. C. Dynes, Transition temperature of strong-coupled superconductors reanalyzed, Phys. Rev. B **12**, 905 (1975).

[17] X. Gonze, B. Amadon, P.-M. Anglade, J.-M. Beuken *et al.*, ABINIT: First-principles approach to material and nanosystem properties, Comput. Phys. Commun. **180**, 2582 (2009).

[18] X. Gonze, F. Jollet, F. Abreu Araujo, D. Adams *et al.*, Recent developments in the ABINIT software package, Comput. Phys. Commun. **205**, 106 (2016).

[19] X. Gonze, B. Amadon, G. Antonius, F. Arnardi *et al.*, The ABINIT project: Impact, environment and recent developments, Comput. Phys. Commun. **248**, 107042 (2020).

[20] C. Hartwigsen, S. Goedecker, and J. Hutter, Relativistic separable dual-space Gaussian pseudopotentials from H to Rn, Phys. Rev. B **58**, 3641 (1998).

[21] S. Baroni, S. D. Gironcoli, A. D. Corso, and P. Giannozzi, Phonons and related crystal properties from density-functional perturbation theory, Rev. Mod. Phys. **73**, 515 (2001).

[22] I. A. Kruglov, D. V. Semenok, H. Song, R. Szczesniak, I. A. Wrona, R. Akashi, M. M. D. Esfahani, D. Duan, T. Cui, A. G. Kvashnin, and A. R. Oganov, Superconductivity of LaH_{10} and LaH_{16} polyhydrides, Phys. Rev. B **101**, 024508 (2020).

[23] I. Errea, F. Belli, L. Monacelli, A. Sanna, T. Koretsune, T. Tadano, R. Bianco, M. Calandra, R. Arita, F. Mauri, and J. A. Flores-Livas, Quantum crystal structure in the 250-K superconducting lanthanum hydride, Nature (London) **578**, 66 (2020).

[24] A. M. Shipley, M. J. Hutcheon, M. S. Johnson, R. J. Needs, and C. J. Pickard, Stability and superconductivity of lanthanum and yttrium decahydrides, Phys. Rev. B **101**, 224511 (2020).

[25] W. Sun, X. Kuang, H. D. J. Keen, C. Lu, and A. Hermann, Second group of high-pressure high-temperature lanthanide polyhydride superconductors, Phys. Rev. B **102**, 144524 (2020).

[26] D. Sun, V. S. Minkov, S. Mozaffari, S. Chariton, V. B. Prakapenka, M. I. Eremets, l. Balicas, and F. F. Balakirev, High-temperature superconductivity on the verge of a structural instability in lanthanum superhydride, Nat. Commun. **12**, 6863 (2021).

[27] C. Wang, S. Yi, and J.-H. Cho, Pressure dependence of the superconducting transition temperature of compressed LaH_{10}, Phys. Rev. B **100**, 060502(R) (2019).

[28] S. Yi, C. Wang, H. Jeon, and J.-H. Cho, Stabilization mechanism of clathrate H cages in a room-temperature superconductor LaH_{10}, Phys. Rev. Mater. **5**, 024801 (2021).

[29] F. Hong, L. Yang, P. Shan, P. Yang, Z. Liu, J. Sun, Y. Yin, X. Yu, J. Cheng, and Z. Zhao, Superconductivity of lanthanum superhydride investigated using the standard four-probe configuration under high pressures, Chin. Phys. Lett. **37**, 107401 (2020).

[30] See Supplemental Material at http://link.aps.org/supplemental/10.1103/PhysRevB.104.214505 for compares the present calculations with previous theoretical predictions and experimental observations for pure LaH_{10}, compares the VCA and supercell results for N-doped LaH_{10}, and presents predicted x-ray diffraction patterns for N-doped LaH_{10}, which is includes Refs. [40,41].

[31] *The Electron-Phonon Interaction in Metals*, edited by E. P. Wohlfahrt, Selected Topics in Solid State Physics Vol. 16 (North-Holland, Amsterdam, 1981).

[32] E. Snider, N. Dasenbrock-Gammon, R. McBride, M. Debessai, H. Vindana, K. Vencatasamy, K. V. Lawler, A. Salamat, and R. P. Dias, Room-temperature superconductivity in a carbonaceous sulfur hydride, Nature (London) **586**, 373 (2020).

[33] Y. Meng, H. K. Mao, P. J. Eng, T. P. Trainor, M. Newville, M. Y. Hu, C. Kao, J. Shu, D. Hausermann, and R. J. Hemley, The formation of sp^3 bonding in compressed BN, Nat. Mater. **3**, 111 (2004).

[34] J. A. Flores-Livas, T. Wang, T. Nomoto, T. Koretsune, Y. Ma, R. Arita, and M. Eremets, Reaching room temperature superconductivity by optimizing doping in LaH_{10}, arXiv:2010.06446.

[35] Y. Sun, J. Lv, Y. Xie, H. Liu, and Y. Ma, Route to a Superconducting Phase Above Room Temperature in Electron-Doped Hydride Compounds Under High Pressure, Phys. Rev. Lett. **123**, 097001 (2019).

[36] H. Wang, Y. Yao, F. Peng, H. Liu, and R. J. Hemley, Quantum and Classical Proton Diffusion in Superconducting Clathrate Hydrides, Phys. Rev. Lett. **126**, 117002 (2021).

[37] S. Di Cataldo, C. Heil, W. von der Linden, and L. Boeri, $LaBH_8$: Towards high-T_c low-pressure superconductivity in ternary superhydride, Phys. Rev. B **104**, L020511 (2021).

[38] X. Liang, A. Bergara, X. Wei, X. Song, L. Wang, R. Sun, H. Liu, R. J. Hemley, L. Wang, G. Gao, and Y. Tian, Prediction of high-T_c superconductivity in ternary lanthanum borohydrides, Phys. Rev. B **104**, 134501 (2021).

[39] P.-W. Guan, R. J. Hemley, and V. Viswanathan, Combining pressure and electrochemistry to synthesize superhydrides, Proc. Natl. Acad. Sci. USA **118**, e2110470118 (2021).

[40] T. B. Boykin, N. Kharche, G. Klimeck, and M. Korkusinski, Approximate bandstructures of semiconductor alloys from tight-binding supercell calculations, J. Phys.: Condens. Matter **19**, 036203 (2007).

[41] P. Larson and S. Satpathy, Supercell studies of the Fermi surface changes in the electron-doped superconductor $LaFeAsO_{1-x}F_x$, Phys. Rev. B **79**, 054502 (2009).